Title:

Central projections of cercal giant interneurons in the adult field cricket, *Gryllus bimaculatus*

Authors:

Hiroki Yamao[1,2,†], Hisashi Shidara[3,4,†], Hiroto Ogawa[3,*]

Running title:

Projections of cricket GIs

Affiliations/Author List Footnotes/Contact info:

1. Department of Biological Sciences, School of science, Hokkaido University, Sapporo 060-0810, Japan

2. Present address: Graduate school of Life Sciences, Tohoku University, Sendai 980-8577, Japan

3. Department of Biological Sciences, Faculty of Science, Hokkaido University, Sapporo 060-0810, Japan

4. Present address: Department of Biochemistry, Graduate school of Medicine, Mie University, Tsu 514-8507, Japan

* corresponding author (E-mail: hogawa@sci.hokudai.ac.jp)

† equal contribution

Data availability statement

There is no specific data available.

Funding statement

This work was supported by JSPS KAKENHI Grant Number 16H06544 (H.O), 18J00589 (H.S.), and 19K16283 (H.S.).

Conflict of interest disclosure

The authors declare no competing interests.

Ethics approval statement

All experiments were conducted in accordance with the Guidelines of the Institutional Animal Care and Use Committee of the National University Corporation, Hokkaido University, Japan, which specify no requirements for the treatment of insects in experiments.

Patient consent statement

Not applicable

Permission to reproduce material from other sources

Not applicable

Clinical trial registration

Not applicable

Acknowledgements

This work was supported by JSPS KAKENHI Grant Number 16H06544 (H.O), 18J00589 (H.S.), and 19K16283 (H.S.).

Graphical abstract

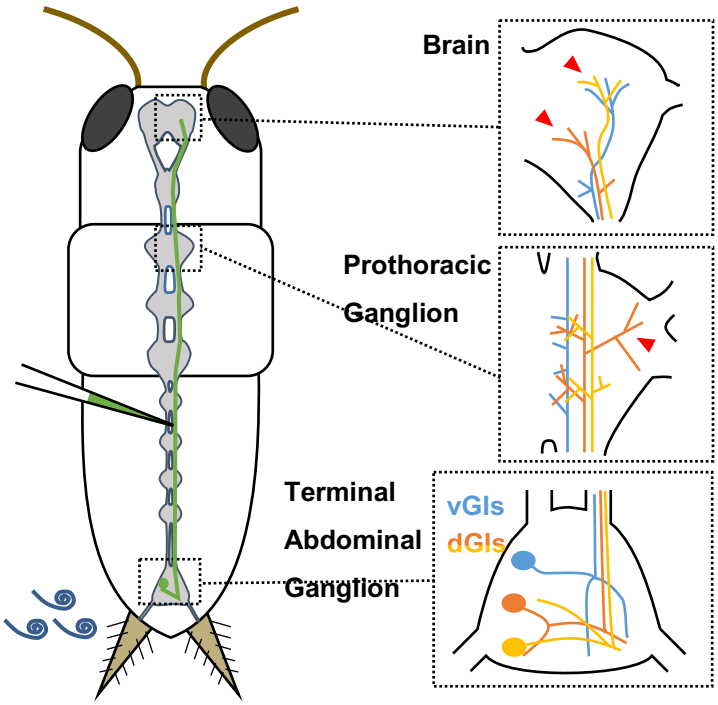

t

Staining six cercal giant interneurons (GIs) in the adult cricket revealed that the projection morphology of ventral and dorsal GIs had distinct characteristics in the brain and the thoracic ganglia, and the dorsal GIs were further divided into two subgroups. These differences likely reflect their physiological properties and behavioral functions.

Abstract

The structures of neurons, such as dendrites and axonal projections, are closely related to their response properties and their specific functions in neural circuits. Identified neurons, having genetically determined morphological features and pre- and postsynaptic partners, play significant roles in specific behaviors. Giant interneurons (GIs) are identified in the terminal abdominal ganglion of the cricket as mechanosensory projection neurons and are sensitive to airflow stimulation of the cerci. GIs are classified into ventral GIs (vGIs) or dorsal GIs (dGIs) depending on the location of their axons running within the connective nerve cord. Based on their response properties to airflow, vGIs are presumed to be involved in triggering the wind-elicited escape response, whereas dGIs are thought to be airflow direction-encoding neurons. The previous findings regarding airflow sensitivity point to possible differences in the morphology of the central projections that may correspond to their neural functions. However, the detailed morphologies of the GIs in the cephalic and thoracic ganglia of adult crickets remain unclear. In this study, we stained six GIs, namely, GI 8-1 (medial giant interneuron, MGI), 9-1 (lateral giant interneuron, LGI), 9-2, 9-3, 10-2, and 10-3, using intracellular iontophoretic or pressure injection of dyes. Staining revealed remarkable differences in the axonal branching patterns between vGIs and dGIs. The dGIs were further divided into subgroups based on the profiles of their axon collaterals and projection sites in the brain. The anatomical differences between the GIs' central projections seemed to be related to their information encodement and behavioral functions.

Keywords

insect, escape behavior, wind stimulus, cercal system, mechanosensory

Key points

- By staining six airflow-sensitive cercal giant interneurons (GIs) in the adult cricket, their anatomical structures in the brain and in the thoracic ganglia were revealed.
- Differences in the axonal arborization patterns of the GIs, not only between dorsal GIs and ventral GIs but also among the dorsal GIs, were elucidated.
- The differences in the projection sites and axon collateral profiles between the GIs seemed to reflect the differences in their neural functions.

1. Introduction

The structures and projections of neurons are closely related to their response properties and information processing characteristics. Therefore, the destination of the projections, along with the physiological activity of neurons, may provide important clues for the analysis of their functions. Various staining methods have revealed the whole morphologies and projection sites of individual neurons, enabling us to predict their computational and behavioral roles (Masland, 2001; D'Angelo et al., 2011). A typical example is seen in the relationship between the response properties of retinal ganglion cells (RGCs) and their projections to the lateral geniculate nucleus (LGN) in the mammalian visual system. Some subtypes of RGCs that have a wide receptive field and high wavelength selectivity project into the magnocellular layer of the LGN, whereas others, which have a narrow receptive field and low wavelength selectivity, connect to the parvocellular layer (Shapley and Hugh Perry, 1986). This segregation is even maintained in the next projection destination, the primary visual cortex (V1) (Livingstone and Hubel, 1988). Another notable example can be observed in the neural circuits of the mammalian cerebellum, which consists of Purkinje cells, parallel fibers of granule cells, and climbing fibers derived from the inferior olive. Purkinje cells, which have characteristic dendrites, receive projections from parallel and climbing fibers in different manners; each granule cell projects onto many Purkinje cells *via* parallel fibers, whereas a single climbing fiber controls only one Purkinje cell (Bell et al., 2008). Such distinct projections of the parallel and climbing fibers to the Purkinje cells

illustrate the difference in their synaptic weights, which underlies the mechanism of long-term depression at synaptic sites between parallel fibers and Purkinje cells (Ito and Kano, 1982; Ito et al., 1982). These examples demonstrate how the axonal projection characteristics of nerve cells are matched to their role in their neural functions.

Identified neurons, such as Mauthner cells in fish, have genetically determined properties in terms of their morphological profiles and connections; therefore, they are useful models for understanding the relationship between an individual neuron's structure and its behavioral function (Korn and Faber, 2005; Schuster, 2012). However, few studies have compared the relationship between the morphology and function of multiple identified neurons at a specific processing stage. Giant interneurons (GIs) are identified as projection neurons in the cricket cercal system, which is considered as a generalist sensory system resembling the mammalian visual or auditory systems (Jacobs et al., 2008). GIs receive excitatory synaptic inputs from a large number of mechanosensory afferents projecting into the terminal abdominal ganglion (TAG) and extract specific information about the surrounding airflow such as flow speed and direction to convey it to higher centers, including the brain. The projections of these sensory afferents form a topographical map, representing airflow direction (Jacobs and Theunissen, 1996). Thus, the dendritic shape of each GI within the afferent map is considered to be closely related to its directional selectivity to the airflow (Jacobs and Theunissen, 2000; Ogawa et al., 2008). According to the developmental features and locations of the axons running

through the ventral nerve cord, GIs are divided into two groups: ventral GIs (vGIs) and dorsal GIs (dGIs) (Jacobs and Murphey, 1987). Although there are slight variabilities between species, vGIs include the medial giant interneuron (MGI, GI 8-1) and the lateral giant interneuron (LGI, GI 9-1), whereas dGIs include GIs 9-2, 9-3, 10-2, and 10-3 (Jacobs and Murphey, 1987; Hirota et al., 1993). From their response properties, vGIs are presumed to be involved in the escape command, whereas dGIs are considered to encode stimulus direction (Kanou and Shimozawa, 1984; Miller et al., 1991; Kohstall-Schnell and Gras, 1994). Among the dGIs, GIs 10-2 and 10-3 are more sensitive compared with GIs 9-2 and 9-3 (Miller et al., 1991), indicating that GIs can be further classified into subgroups based not only on the location of their axons but also on their physiological properties and computational functions. This implies that the characteristics of the GIs' axonal projections, including collaterals in the brain and the thoracic ganglia, could vary depending on their axon-running location and response properties. However, the detailed projections of the GIs in the brain and other ganglia of adult crickets are still unclear, despite the whole morphology of the GIs having been descriptively investigated in third instars (Hirota et al., 1993).

In this study, we examined the projection sites and arborizations of six representative airflow-sensitive GIs in adult crickets. To reveal the detailed morphology of each GI in the cephalic and thoracic ganglia, we obtained a series of optical slice images of the GIs stained with a fluorescent dye. Based on these images, the gross morphology of the GIs was reconstructed. We found that the

structures in adult crickets essentially had the same characteristics as in the third instars. Our analysis also revealed various differences in the axonal arborization patterns in the brain among the distinct GIs. Such differences were observed not only between subgroups (the dGIs and vGIs) but also between different dGIs. The differences in the projection regions and axon collateral profiles of the GIs are likely related to their neural functions.

2. Materials and methods

2.1 Animals

Laboratory-bred adult male crickets (*Gryllus bimaculatus*, Hokudai WT; Watanabe et al., 2018) 1–2 weeks after imaginal molting were used in all experiments. Crickets were reared under 12:12-h light/dark conditions at a constant temperature of 28℃.

2.2 Electrophysiology for dye loading into single cells

To prepare for the electrophysiological recordings, crickets, anesthetized on ice in advance, were pinned dorsal side up on a silicone platform after the wings and legs were removed. To expose the TAG, an incision was made along the dorsal midline of the abdomen, and the guts, together with the surrounding fat, were removed. Intracellular recordings were conducted using a glass electrode filled with either 4% Lucifer yellow CH potassium salt (Thermo Fisher) or 1% Alexa Fluor 568 Hydrazide

(Thermo Fisher) diluted in 200-mM potassium acetate. The resistance of the electrodes was set to either 15–30 or 80 MΩ, depending on the region of the GI being recorded. The electrodes with the resistance of 80 MΩ were inserted into the dendrites of the GIs in the TAG, and those with the resistance of 15–30 MΩ were inserted into the axons of the GIs in the connective nerve cord between the second and third abdominal ganglia. To evoke action potentials in the GIs, which could be easily identified electrophysiologically, the sensory afferents ipsilateral to the axons of the recorded GIs were stimulated by an electrical pulse with a 50-μs duration using a hook electrode. The GI's membrane potential was measured, and the signal was amplified using an amplifier (MEZ-8300, NIHON KOHDEN). After the successful insertion of the electrodes, a hyperpolarizing current of either 3 or 25 nA was injected into the GIs by the electrode with higher or lower resistance, respectively, for a maximum of 60 min. After the current injections, the samples were kept at 4°C for a minimum of 48 h to allow the dye to spread to the axon terminals.

2.3 Random dye loading into giant interneurons (GIs)

To randomly stain the GIs, fluorescent dye was pressure-injected into the ventral nerve cord (VNC). In preparation, crickets anesthetized with ice were fixed ventral side up on a silicone platform. A small part of the second-to-third segmental sternum was removed to expose the VNC. A glass micropipette filled with the dye solution, which contained 1% Alexa Fluor 488 dextran conjugates (10,000 MW) or

1% Alexa Fluor 594 dextran conjugates (10,000 MW) (Thermo Fisher) diluted in distilled water, was inserted into the VNC. Approximately 20–50 nL of the dye solution was manually pressure-injected into one or both of the VNCs using a plastic syringe connected to the micropipette. Then, the removed sternum piece was placed back on the exposed ventral area and covered with paraffin jelly. The treated crickets were kept for 3–5 days with free access to food and water, allowing the dye to spread to the dendrites and axon terminals. The number of stained neurons varied depending on the amount of dye solution injected, but in most cases, only single GIs were stained. When double-staining multiple GIs with different dyes, two micropipettes filled with Alexa Fluor 488 and 594 were inserted into different locations in the VNC.

2.4 Two-photon imaging of GIs

After the dye had spread, the brain and ganglia were isolated; fixed in 4% paraformaldehyde in 200-mM phosphate buffer for 3 h; dehydrated for 7 min in 50% and 70% ethanol and for 10 min in 90%, 100%, and 100% ethanol; and then cleared in methyl salicylate. Fluorescence images were obtained using a two-photon upright microscope (FLUOVIEW FV1000MPE, Olympus) with 10×/0.50-NA objective lens (Fluar, ZEISS). For excitation of the fluorescent dyes, the wavelength of the two-photon laser was adjusted as follows: 860 nm for Lucifer yellow CH, 800 nm for Alexa Fluor 568 and 594, and 760 nm for double-staining with Alexa Fluor 488 and 594. To obtain the fluorescence of Lucifer

yellow CH, a 570-nm sharp-cut dichroic mirror (SDM) and the 495–540-nm emission filters were used. The fluorescence of the other combinations of dyes was obtained using a 570-nm SDM and 495–540- and 575–630-nm emission filters. The xy resolution of each image was 1.242 μm/pixel, and the z-step was 2 μm. To acquire three-dimensional (3D) data from the GIs, a series of images were obtained at ~1024 × ~1024 pixels in ~240 z-steps (i.e., a volume of ~1272 × ~1272 × ~480 μm).

2.5 Analysis of imaging data

Image processing, including the tracing and 3D reconstruction of GIs, was conducted using the ImageJ and NeuTube software (Feng et al., 2015). First, the morphology of each GI was obtained from a series of images of samples in which a single GI was stained. GIs were identified from their dendritic shapes and locations of their somata in the TAG. Using NeuTube, the neurites, axons, and collaterals of the GIs were traced semiautomatically. After the morphology of the GIs was determined, the samples in which multiple GIs were stained were analyzed in the same way to elucidate the relative positions between the GIs. For these multistained samples, each labeled neuron was identified from the morphological features of each ganglion by referring to the data obtained from the single-stained samples. If two neurons were located too close in proximity to be distinguished in the fluorescent image, they were designated as simply vGIs or dGIs. All images presented in the figures, except Figure 1, were 3D-reconstructed. Since the point of view in this 3D-reconstruction process was adjusted

manually to observe the ganglia from the ventral or lateral side, the scale bars could not be indicated in those images.

To measure the spread of the axon terminals of MGI and LGI in the deutocerebrum, the optical slices that include the most dorsal and most ventral edges of their axonal branches were identified, and the dorsoventral distance was calculated based on the number of the optical slices between those slices. In the sample where both MGI and LGI were observed, we calculated the spread of these cells together because it was difficult to discriminate their axon terminals. Furthermore, the lengths of the small medial branch of LGI in the posterior regions of the deutocerebrum and of the lateral branches of GIs 9-2 and 9-3 in the prothoracic ganglia were measured as the mediolateral distance between the branching points to their edges. Also, the lengths of the ventral branches of GIs 10-2 and 10-3 in the brain, extending perpendicularly to the dorsally positioned branches, were measured in the dorsoventral direction based on the number of the optical slices between the branching point and the edge of the ventral branches. Samples in which fluorescent images were unclear or some axon branches could not be observed were excluded from the calculations. The morphological values given in the text indicate the mean ± SD of the measured samples.

The nomenclature of the insect brain and axes following the description given by the Insect Brain Name Working Group (Ito et al., 2014) was adopted. Here, the gnathal ganglion (GNG) corresponds to the suboesophageal ganglion (SOG), which has usually been used in previous cricket

studies.

3. Results

3.1 Whole morphology of six airflow-sensitive GIs

To examine the whole morphology of the GIs, we stained them with fluorescent dyes *via* intracellular iontophoretic or pressure injection. The stained samples allowed us to observe the whole structure of GIs throughout the cricket central nervous system (Fig. 1). In this study, we succeeded in obtaining clear images of six GIs, namely, MGI, LGI, GI 9-2, GI 9-3, GI 10-2, and GI 10-3 in multiple samples (Fig. 2, Table 1). The representative results are shown in the figures, and the morphological features of each GI described below were commonly observed across most of the samples we obtained (Table 1). All GIs ascended their axons through a connective of the nerve cord from the TAG to the deutocerebrum (Figs. 3 and 4). The ascending axons arborized with collaterals in all ganglia, and the collaterals did not extend across the midline into the contralateral hemisphere (Figs. 5, 6, and 7). The axons of the dGIs (GIs 9-2, 9-3, 10-2, and 10-3) traveled through the dorsal tract within the nerve cord, while those of the vGIs (MGI and LGI) did so through the ventral tract (Fig. 7). In addition, the dGIs extended their axon collaterals medially and laterally in each thoracic ganglion, whereas those of the vGIs only did so medially (Figs. 5 and 6). These morphological features were consistent with those in the third instars reported in a previous study (Hirota et al., 1993). Subsequently, the details of the

central projections of each GI in the cephalic and thoracic ganglia were further analyzed.

3.2 Dendritic arborizations in the terminal abdominal ganglion

Each GI showed distinct and unique dendritic structures in the TAG, and their dendritic arborizations were commonly observed across all the multiple samples that we obtained (Fig. 2). All GIs extended their axons contralaterally to their somata. The somata of GIs 9-2 and 10-2 were located at the ventral side of the TAG, whereas that of GI 9-3 was positioned at the dorsal side. For the MGI, LGI, and GI 10-3, the somata were located approximately in the center of the dorsoventral axis. Dendrites of the MGI, LGI, and GI 9-2 were restricted to the axon-side hemisphere, whereas GIs 9-3, 10-2, and 10-3 had dendrites in both hemispheres. The MGI had two large dendritic branches with many short subbranches, with the medial branch located more ventrally than the lateral branch. Most of the LGI's dendrites extended dorsally and were concentrated in the small posterior region of the TAG. Like the MGI, GI 9-2 had two large dendrites at the contralateral side to its soma, from which many small subbranches extended to the ventral side of the TAG. Additional small branches occurred medially and ventrally. GI 9-3 exhibited characteristic neurite shapes with three main dendrites, two of which extended laterally or posteriorly at the soma side; the other was located posteriorly on the axon side. The axon of GI 9-3 was positioned at the dorsal side of the TAG, and most of the dendrites, including the main branches, extended ventrally. GI 10-2 extended its dendrites from the main neurite in the

dorsoventral axis. The dendrites of GI 10-2 included three large branches, two of which extended dorsoventrally from the main neurite on the axon side; the other branch extended more ventrally near the soma. The axon and dendrites of GI 10-2 were medially concentrated and relatively compact compared with those of the other GIs. GI 10-3 also had three large dendrites extending from a posterolateral site of the axon. One of these divided further into many small dendrites, which were concentrated near the junction. Another dendrite extended to the soma side and arborized more anteriorly, while the third dendrite was located close to the soma. The dGIs have two common characteristics: their axons were positioned dorsally in the TAG, and all dendrites extended more ventrally than the axon.

3.3 Central projections of the GIs in the brain

The axons of all the GIs projected to the brain and exhibited characteristic arborizations of axon terminals in the deutocerebrum (Fig. 3). Those features were consistent across all samples. The axons of the GIs entered the brain at the dorsal side through the connective. The axons of the MGI and LGI branched off in the middle of the dorsoventral axis, and their collaterals were extended both dorsally and ventrally, of which the dorsoventral spread was 188.0 ± 92.7 μm (N = 17). The LGI also had small medial branches, of which the mediolateral length was 82.1 ± 26.9 μm (N = 14), in the posterior regions of the deutocerebrum. Both GI 9-2 and GI 9-3 arborized at the dorsal side of the

brain with lateral collaterals that branched in a relatively sparse manner. The larger axonal arborizations extended medially and the smaller ones posteriorly. The axonal arborizations of GIs 10-2 and 10-3 had an L-shaped structure, which consisted of the dorsal branches extending anteriorly in parallel to the axon and the ventral branches extending perpendicularly to the dorsal branches, of which the dorsoventral width was 139.0 ± 45.8 μm (N = 8). The ventral branches of GI 10-2 extended medially in proximity to the central-body complex.

To identify the relative positions of the axon terminals among GIs in the brain, we studied their branches in several samples where multiple GIs were simultaneously stained (Fig. 4, Table 1). When there were difficulties in distinguishing between separate branches due to overlapping in the fluorescent images, we designated them as simply vGIs or dGIs (Figs. 4 and 7). For the GIs within either the vGI or dGI group, the axons of the GIs ran along the same route and branched at similar sites. Dorsal GIs, such as GIs 9-2, 9-3, and 10-2, had axon collaterals more medio-posteriorly than vGIs (Fig. 4). However, even within the same group, there were differences in the details of the locations of the axon terminals. The axon collaterals of GIs 9-2 and 9-3 were positioned more medially compared with those of the LGI (Fig. 4a, b), whereas those of GI 10-2 were in close proximity to those of the LGI (Fig. 4c). Interestingly, the axonal arborizations of the MGI and LGI were located between the two orthogonally extended axonal branches of GI 10-2 (Fig. 4c, d). The posterior branches of the LGI and GI 9-3, which belong to different groups, were located at the same region, whereas GI 9-2,

which is in the same group as GI 9-3, lacked posterior branches (Fig. 4a, b, and d). The existence of these branches suggests that the axon collaterals of multiple GIs are most likely concentrated in a specific site of the posterior brain region. Such relationships between the axon collateral locations of the GIs were also consistent in the other samples where multiple GIs were stained (Table 1). Taken together, the branching patterns of the GIs' axon terminals were unique to each cell while also having some common features within the vGIs and dGIs groups. Moreover, based on the morphological characteristics in the branching patterns of the GIs' axons, the six GIs we studied could be categorized into three groups: (1) MGI and LGI, (2) GIs 9-2 and 9-3, and (3) GIs 10-2 and 10-3. This classification based on morphology could reflect differences in the neural functions of these GIs, as outlined in the Discussion.

3.4 Projections of axon collaterals in other segmental ganglia

All GIs had medial axon collaterals in the gnathal, prothoracic, mesothoracic, and metathoracic ganglia, which were observed in all samples (Figs. 5 and 6). For all GIs, the more posterior the ganglion in the thorax, the greater the number of axon collaterals. Ventral GIs, such as the MGI and LGI, had short axon collaterals that extended medially in the same dorsoventral plane as their axons (Fig. 5). On the contrary, the dGIs (GIs 9-2, 9-3, 10-2, and 10-3) had long collaterals both medially and laterally at different depths relative to their axons (Fig. 6). We found that the pattern of axon

collaterals in the GIs differed between the gnathal and thoracic ganglia. In the GNG, the vGIs had four to six collaterals of similar sizes (4.8 ± 0.8 collaterals in MGI, N = 5; 4.3 ± 0.5 collaterals in LGI, N = 9), whereas the posterior branches of the dGIs were larger and more highly branched than their anterior counterparts. The most remarkable feature specific to the thoracic ganglia was that GIs 9-2 and 9-3 extended characteristic long lateral collaterals dorsally. These collaterals extended 251.0 ± 36.2 μm in GI 9-2, N = 8; 186.0 ± 67.4 and 239.0 ± 24.5 μm in GI 9-3, N = 8 and 9 for the anterior and posterior collaterals, respectively, in the mediolateral direction. On the contrary, the collaterals of GIs 10-2 and 10-3 were concentrated centrally in the anteroposterior axis and extended ventrally. The MGI and LGI had small branches extending only medially (5.0 ± 1.1 collaterals in MGI, N = 8; 3.2 ± 0.8 collaterals in LGI, N = 13). These features were observed in both the prothoracic ganglion (PTG) and mesothoracic ganglion (MsTG) and were also common for the GNG. In the metathoracic ganglion (MtTG), GIs 9-2 and 9-3 also extended long lateral branches. In addition, almost every GI seemed to extend larger numbers of axon collaterals with dense branches medially in the MtTG than in the PTG and MsTG. For example, the MGI had 5, 10, or 11 medial collaterals (N = 3) in the MtTG, while it had 5.0 ± 1.1 in the PTG (N = 8) and 5.8 ± 1.7 in the MsTG (N = 4).

As with the brain, we also investigated the relative positions of the GIs' axon collaterals in the segmental ganglia in samples where multiple GIs were simultaneously stained (Fig. 7). We designated the stained axons as those of the vGIs as it was difficult to distinguish between the MGI

and LGI's axon. In both of these samples, as referred to by their group names, the axons of the MGI and LGI passed ventrally through the ganglia, whereas those of GIs 9-2, 9-3, and 10-2 passed dorsally. Although the axon collaterals of the dGIs were widely branched along the dorsoventral axis, they did not extend to the proximity of the vGIs. Even so, the medial branches of the GIs were in close range to each other. These characteristics in the relative location of the GIs' axonal collaterals in gnathal and thoracic ganglia were consistent across the samples where multiple GIs were stained. This suggests that the medial regions of the GIs' axons are common output sites, where the neural circuits in the gnathal and thoracic ganglia may receive synaptic inputs from GIs.

4. Discussion

In the cercal system of the cricket, GIs receive excitatory synaptic inputs from the mechanosensory hairs that detect the surrounding airflow and they generate spikes propagating into higher centers, including the brain and thoracic ganglia (Jacobs et al., 2008). The response characteristics of the GIs to airflow stimuli have been well investigated and imply the GIs' roles in airflow signal processing and stimulus-evoked behaviors (Oe and Ogawa, 2013). Since neuronal functions are closely related to the morphology of neurons in general, we investigated the axonal projections of GIs in the brain and the other segmental ganglia to understand the differences in their functional roles. We found that there were morphological differences in axonal projections between the vGIs and dGIs, as well as common

characteristics within each cell group. Furthermore, there were distinctive differences even among the dGI cells. This result indicated that dGIs could be categorized into further subgroups in terms of their morphological structures and therefore implied how each subgroup may play different physiological roles as discussed below.

A previous study demonstrated that eight GIs have projections to the brain in third-instar crickets (Hirota et al., 1993). However, the developmental changes in hemimetabolous insects can result in alterations in the axonal arborization structures (Boyan, 1983). Our study indicated that the relative positions of the GIs' axonal projections in the thoracic ganglions and brains of adult crickets are consistent with those in third-instar larvae, suggesting that no drastic changes in the structures of the GIs occur during maturation. In fact, the innate escape behavior mediated by the GIs are fully maturated 24 h after the imaginal molt (Sato et al., 2017). Therefore, even considering the drastic morphological changes during development, including wing formation, it is unlikely that the morphology and behavioral roles of GIs are changed during the imaginal molt. In addition, although the GIs' morphology slightly differed in the details among different samples, the number and locations of the primary large branches extending from the axon were consistent across the samples (Figs. 3-7). At least the characteristics reported in this study were confirmed in multiple samples (Table 1). Thus, the morphological characteristics of the cricket cercal GIs are likely to be strongly conserved throughout the developmental process.

How do these projection patterns of the GIs relate to their neural functions? In the brain, the branching points of the axon terminals were different between the vGIs and dGIs. Furthermore, the detailed arborization patterns beyond the branching points distinctively varied even among the dGIs. GIs 9-2 and 9-3 projected their branches at a medial-posterior site, whereas GI 10-2 was positioned relatively close to the LGI and MGI. Unfortunately, we could not obtain a double-stained sample of GI 10-3, the MGI, or the LGI. However, the anatomical features of GI 10-3 were similar to those of GI 10-2, suggesting that GI 10-3 is also located close to the MGI and LGI. GIs 10-2 and 10-3 especially contribute to the encoding of the direction of air currents (Miller et al., 1991), whereas the MGI and LGI are possibly involved in the escape command (Kanou and Shimozawa, 1984). The escape behavior of crickets in response to airflow stimuli is precisely controlled *via* neural processing in the brain, allowing them to move in the opposite direction of the stimulus (Oe and Ogawa, 2013; Sato et al., 2019). To accurately control this escape behavior, crickets have to detect the direction and velocity of the air currents and regulate their motor outputs accordingly (Sato et al., 2021). The sensory information about air currents could be processed and integrated at the brain region where the axon terminals of the LGI, MGI, GIs 10-2, and 10-3 are concentrated. In the TAG, the stimulus direction is topographically represented by sensory afferents, from which GIs 10-2 and 10-3 extract directional information to produce their distinct directional sensitivities (Jacobs and Theunissen, 1996, 2000; Ogawa et al., 2008). Conversely, in the brain, although GIs 10-2 and 10-3 had remarkable ventral

branches of axon terminals, no significant difference between their locations was observed. Thus, the airflow direction may not be topographically represented in the brain, unlike in the TAG.

A clear difference was observed in the axonal projections within the thoracic ganglia between the subgroups of GIs: the dGIs had lateral branches of their axonal collaterals in addition to the medial branches extending dorsally or ventrally relative to their axons, whereas the vGIs had only medial branches extending in the same dorsoventral plane as their axons. Moreover, the lateral branches of GIs 9-2 and 9-3 extended to the lateral regions of each ganglion. Depolarizing currents injected into dGIs elicit leg movements (Hirota et al., 1993), suggesting that the lateral branches of the dGIs provide excitatory synaptic inputs to motor neurons. Furthermore, current injections into GIs 9-2 and 9-3 induce leg movements with a shorter delay than those into GIs 10-2 and 10-3 (Hirota et al., 1993). GIs 9-2 and 9-3 also encode airflow direction, but their sensitivity to air current stimuli is lower than that of GIs 10-2 and 10-3 (Kanou and Shimozawa, 1984; Miller et al., 1991). Considering the differences in the projection patterns of GIs 9-2 and 9-3 compared with other GIs in the brain and thoracic ganglia, GIs 9-2 and 9-3 may play a role in triggering escape behaviors in response to stronger airflow stimuli. The lateral branches of GIs 9-2 and 9-3 in the thoracic ganglia possibly have direct synaptic contacts with thoracic motor neurons. Interestingly, the antennal giant interneurons, which are mechanosensitive descending projection neurons in the brain, share similar morphological features to those of the cercal GIs. DBNi1-2 has only medial axon collaterals in the thoracic ganglia, whereas

DBNc1-2, DBNc2-2, and DBNi2-1 have both medial and lateral collaterals (Schöneich et al., 2011). These antennal giant interneurons that have lateral collaterals may be directly linked to leg motor neurons in thoracic ganglia (Baden and Hedwig, 2008; Schöneich et al., 2011); thus it is also plausible that the lateral axonal projection of the cercal GIs may also be connected to the motor neurons.

Although current injections into the stationary cricket vGIs induce no behavioral responses (Hirota et al., 1993), hyperpolarization of the LGI during the crickets locomotion induces a rotation to the axonal side of the LGI (Gras and Kohstall, 1998). In cockroaches, stimulation of any of the vGIs triggers a weak response in the motor neurons (Ritzmann and Camhi, 1978). It has also been reported that the vGIs in cockroaches have synaptic contacts with thoracic interneurons *via* their ventral medial branches (Ritzmann and Pollack, 1990). Thus, the medial branches of the GIs in the thoracic ganglia possibly provide synaptic inputs to local interneurons, indirectly activating motor neurons. The activation of the motor neurons *via* such neural circuits, connected to the GIs' medial branches, may be involved in the preparatory tensing of leg muscles for the escape behavior. In addition, an auditory projection neuron, AN2, located in the prothoracic ganglion, responds to airflow stimuli, suggesting some input to it from the cercal system (Someya and Ogawa, 2018). The medial branches of GIs could also be connected with other interneurons, including the ascending neurons in the thoracic ganglia. However, the synaptic connections between the GIs and the thoracic motor neurons or the local interneurons remain unclear, as well as their contributions to specific behaviors.

In other species of orthoptera that have cercal organs, the giant interneurons also have been identified as ascending projection neurons in the TAG. The cercal GI's morphologies in the TAG of the house cricket, *Acheta domesticus*, are very similar to those of the field cricket, *Gryllus bimaculatus,* used in this study. Furthermore, the positional relationships between GIs in both the dorsal-ventral and medial-lateral axes were commonly shared between both species (Mendenhall and Murphey, 1974). However, the arborization patterns of the axonal collaterals differed between the two species. Lateral collaterals of the LGI (GI 9-1) and MGI (GI 8-1) in the MsTG and MtTG, reported in *Acheta domesticus,* were not observed in *Gryllus bimaculatus*. Contrary to this, the LGI and MGI of *Acheta domesticus* had both medial and lateral axonal collaterals in these ganglia (Mendenhall and Murphey, 1974). Furthermore, in the bush cricket, *Tettigonia cantas*, the morphology of the cercal GIs largely differs from those of other species of crickets, and seems to be relatively similar to those seen in cockroaches (Shen, 1983; Collin, 1985). Also, a commonality in orthoptera were that some types of the cercal giant interneurons only have medial collaterals, while others have both medial and lateral collaterals (Shen, 1983; Stubblefield and Comer, 1989). Such morphological differences between giant interneurons may reflect their physiological properties and behavioral functions. Thus, these giant interneurons could be classified into subgroups also in other species, apart from *Gryllus bimaculatus.*

Cercal GIs have been identified for a few decades; therefore, their morphology in the TAG and the physiological characteristics in response to air flow dynamics have been well studied (Jacobs

et al., 2008). Thus, their possible anatomy–function relationships could be discussed in detail. In mammalian visual and motor systems, the dendritic/axonal structures of individual neurons and their projecting sites correspond to their functions in neural processing (Masland, 2001; D'Angelo et al., 2011). The results in this study indicated the correspondence of the central projections with the response properties of GIs, suggesting "labor division" in the GI system for cercal-mediated behavior. The cercal system of crickets is considered to be a generalized sensory system, similar to the visual and auditory systems (Jacobs et al., 2008). The elucidation of the neural circuits postsynaptic to the GIs, therefore, could help us understand the whole picture of neural systems mediating the entire process from sensory perception to behavioral control, across animal species. The wind-elicited escape behaviors of crickets are dependent on the integration of multiple parameters of airflow stimulus information, including velocity and direction, which could be encoded by the population vector of the activity of four GIs (Levi and Camhi, 2000a; b). Comprehensive insights into both the morphology and computational functions of identified neurons could provide the answer to how the neural system "decodes" and integrates the multiple sensory cues represented by the population activity.

References

Bell CC, Han V, Sawtell NB. 2008. Cerebellum-like structures and their implications for cerebellar function. Annu Rev Neurosci 31:1–24.

Boyan GS. 1983. Postembryonic development in the auditory system of the locust. J Comp Physiol 151:499–513.

Collin SP. 1985. The central morphology of the giant interneurons and their spatial relationship with the thoracic motorneurons in the cockroach, *Periplaneta americana* (Insecta). J Neurobiol

D'Angelo E, Mazzarello P, Prestori F, Mapelli J, Solinas S, Lombardo P, Cesana E, Gandolfi D, Congi L. 2011. The cerebellar network: from structure to function and dynamics. Brain Res Rev 66:5–15.

Feng L, Zhao T, Kim J. 2015. neuTube 1.0: A New Design for efficient neuron reconstruction software based on the SWC format. eNeuro 2:ENEURO.0049-14.2014.

Hirota K, Sonoda Y, Baba Y, Yamaguchi T. 1993. Distinction in morphology and behavioral role between dorsal and ventral groups of cricket giant interneurons. Zoolog Sci 10:705–709.

Ito K, Shinomiya K, Ito M, Armstrong JD, Boyan G, Hartenstein V, Harzsch S, Heisenberg M, Homberg U, Jenett A, Keshishian H, Restifo LL, Rössler W, Simpson JH, Strausfeld NJ, Strauss R, Vosshall LB. 2014. A systematic nomenclature for the insect brain. Neuron 81:755–765.

Ito M, Kano M. 1982. Long-lasting depression of parallel fiber-Purkinje cell transmission induced by conjunctive stimulation of parallel fibers and climbing fibers in the cerebellar cortex. Neurosci Lett 33:253–8.

Ito M, Sakurai M, Tongroach P. 1982. Climbing fibre induced depression of both mossy fibre responsiveness and glutamate sensitivity of cerebellar Purkinje cells. J Physiol 324:113–34.

Jacobs GA, Miller JP, Aldworth Z. 2008. Computational mechanisms of mechanosensory processing in the cricket. J Exp Biol 211:1819–1828.

Jacobs GA, Murphey RK. 1987. Segmental origins of the cricket giant interneuron system. J Comp Neurol 265:145–57.

Jacobs GA, Theunissen FE. 1996. Functional organization of a neural map in the cricket cercal sensory system. J Neurosci 16:769–84.

Jacobs GA, Theunissen FE. 2000. Extraction of sensory parameters from a neural map by primary sensory interneurons. J Neurosci 20:2934–43.

Kanou M, Shimozawa T. 1984. A threshold analysis of cricket cercal interneurons by an alternating air-current stimulus. J Comp Physiol A 154:357–365.

Kohstall-Schnell D, Gras H 1994. Activity of giant interneurones and other wind-sensitive elements of the terminal ganglion in the walking cricket. J Exp Biol 193(1), 157–181.

Korn H, Faber DS. 2005. The Mauthner cell half a century later: A neurobiological model for decision-making? Neuron 47:13–28.

Levi R, Camhi JM. 2000a. Population vector coding by the giant interneurons of the cockroach. J Neurosci 20:3822–3829.

Levi R, Camhi JM. 2000b. Wind direction coding in the cockroach escape response: Winner does not take all. J Neurosci 20:3814–3821.

Livingstone M, Hubel D. 1988. Segregation of form, color, movement, and depth: anatomy, physiology, and perception. Science 240:740–9.

Masland RH. 2001. The fundamental plan of the retina. Nat Neurosci 4:877–86.

Mendenhall B, Murphey RK. 1974. The morphology of cricket giant interneurons. J Neurobiol 5:565–580.

Miller JP, Jacobs GA, Theunissen FE. 1991. Representation of sensory information in the cricket cercal sensory system. I. Response properties of the primary interneurons. J Neurophysiol 66:1680–9.

Oe M, Ogawa H. 2013. Neural basis of stimulus-angle-dependent motor control of wind-elicited walking behavior in the cricket Gryllus bimaculatus. PLoS One 8:e80184.

Ogawa H, Cummins GI, Jacobs G a, Oka K. 2008. Dendritic design implements algorithm for synaptic extraction of sensory information. J Neurosci 28:4592–603.

Ritzmann RE, Camhi JM. 1978. Excitation of leg motor neurons by giant interneurons in the cockroach Periplaneta americana. J Comp Physiol 125:305–316.

Ritzmann RE, Pollack AJ. 1990. Parallel motor pathways from thoracic interneurons of the ventral giant interneurons system of the cockroach, Periplaneta americana. J Neurobiol 21:1219–1235.

Sato N, Shidara H, Ogawa H. 2017. Post-molting development of wind-elicited escape behavior in the cricket. J Insect Physiol 103:36–46.

Sato N, Shidara H, Ogawa H. 2019. Trade-off between motor performance and behavioural flexibility in the action selection of cricket escape behaviour. Sci Rep 9:1–13.

Sato N, Shidara H, Ogawa H. 2021. Action selection based on multiple-stimulus aspects in the wind-elicited escape behavior of crickets. bioRxiv:2021.04.23.441064.

Schuster S. 2012. Fast-starts in hunting fish: Decision-making in small networks of identified neurons. Curr Opin Neurobiol 22:279–284.

Shapley R, Hugh Perry V. 1986. Cat and monkey retinal ganglion cells and their visual functional roles. Trends Neurosci 9:229–235.

Shen J-X. 1983. The cercus-to-giant interneuron system in the bushcricket *Tettigonia cantans*: Morphology and response to low-frequency sound. J Comp Physiol 151:449–459.

Someya M, Ogawa H. 2018. Multisensory enhancement of burst activity in an insect auditory neuron. J Neurophysiol 120:139–148.

Stubblefield GT, Comer CM. 1989. Organization of giant interneuron projections in thoracic ganglia of the cockroach *Periplaneta americana*. J Morphol 200:199–213.

Watanabe T, Ugajin A, Aonuma H. 2018. Immediate-Early Promoter-Driven Transgenic Reporter System for Neuroethological Research in a Hemimetabolous Insect. eNeuro 5.

Figure legends

Figure 1. Fluorescence images showing the complete projection pattern of the lateral giant interneuron (LGI) in the central nervous system of an adult cricket. Each image was constructed *via* projection of approximately 240 optical slices acquired at different planes using a two-photon microscope. Abbreviations: GNG, gnathal ganglion; PTG, prothoracic ganglion; MsTG, mesothoracic ganglion; MtTG, metathoracic ganglion; TAG, terminal abdominal ganglion. In conventional cricket studies, the GNG is denoted as the suboesophageal ganglion (SOG), but the nomenclature introduced by Ito et al. (2014) is followed here. All images are shown in the same scale.

Figure 2. Morphology of six giant interneurons (GIs) in the terminal abdominal ganglion. The green traces indicate a 3D image of the GIs built from an optical stack. Abbreviations: A, neuraxis-anterior; P, neuraxis-posterior; V, neuraxis-ventral; D, neuraxis-dorsal.

Figure 3. Axon collaterals and terminals of GIs in the brain. (See Figure 2 legend for abbreviations.) The magenta lines and arrows indicate the mediolateral and dorsoventral lengths referred to in Results.

Figure 4. Relative positions of GI axon terminals in the brain. The colors indicate the morphology for different GIs. The projections were identified based on morphological cues for each GI obtained in

the brain and other ganglia. GI 9-1b in (b) was classified as a ventral GI (vGI) and identified according to its morphological features in the other ganglia. The axon terminals in (d) designated as dorsal GIs (dGIs) included GIs 9-3 and 10-2, and those designated as vGIs included the LGI and the medial giant interneuron (MGI), but they could not be identified as specific GIs. (See Figure 2 legend for abbreviations.)

Figure 5. Axon collaterals of the MGI and LGI in the gnathal, prothoracic, mesothoracic, and metathoracic ganglia. (See Figure 2 legend for abbreviations.)

Figure 6. Axon collaterals of GIs 9-2, 9-3, 10-2, and 10-3 in the gnathal, prothoracic, mesothoracic, and metathoracic ganglions. (See Figure 2 legend for abbreviations.) The magenta lines and arrows indicate the mediolateral length referred to in Results.

Figure 7. Relative positions of GI axon collaterals in the gnathal, prothoracic, mesothoracic, and metathoracic ganglia. The images in (a) and (b) were obtained from the same samples as Fig. 4a and d. The blue axons shown in (a-i) and (a-iv) were designated as vGIs as it was difficult to separate them into MGI or LGI. For the sample shown in (b), the images from the mesothoracic and metathoracic ganglia are not shown because the projections of many neurons were concentrated and overlapping,

and it was difficult to divide them into vGIs or dGIs. (See Figure 2 legend for abbreviations.)

Table 1. Number of samples analyzed in this study.

Figure 1

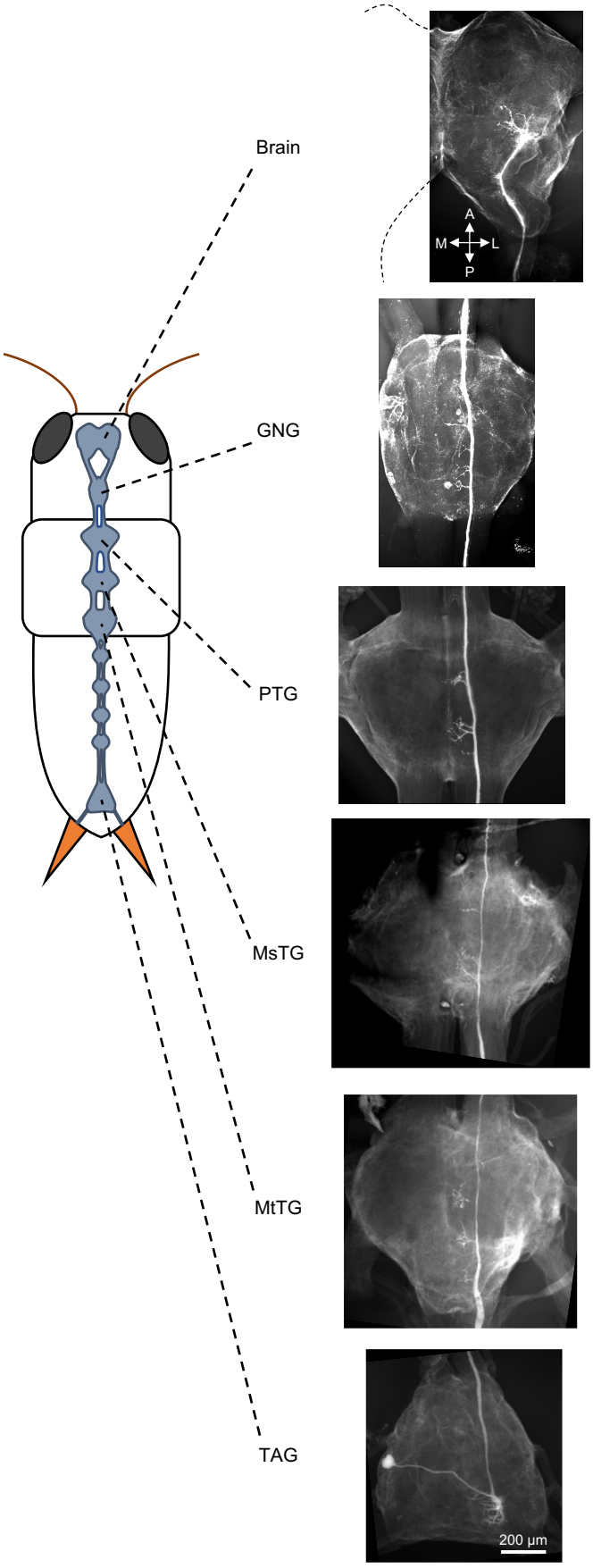

Figure 2

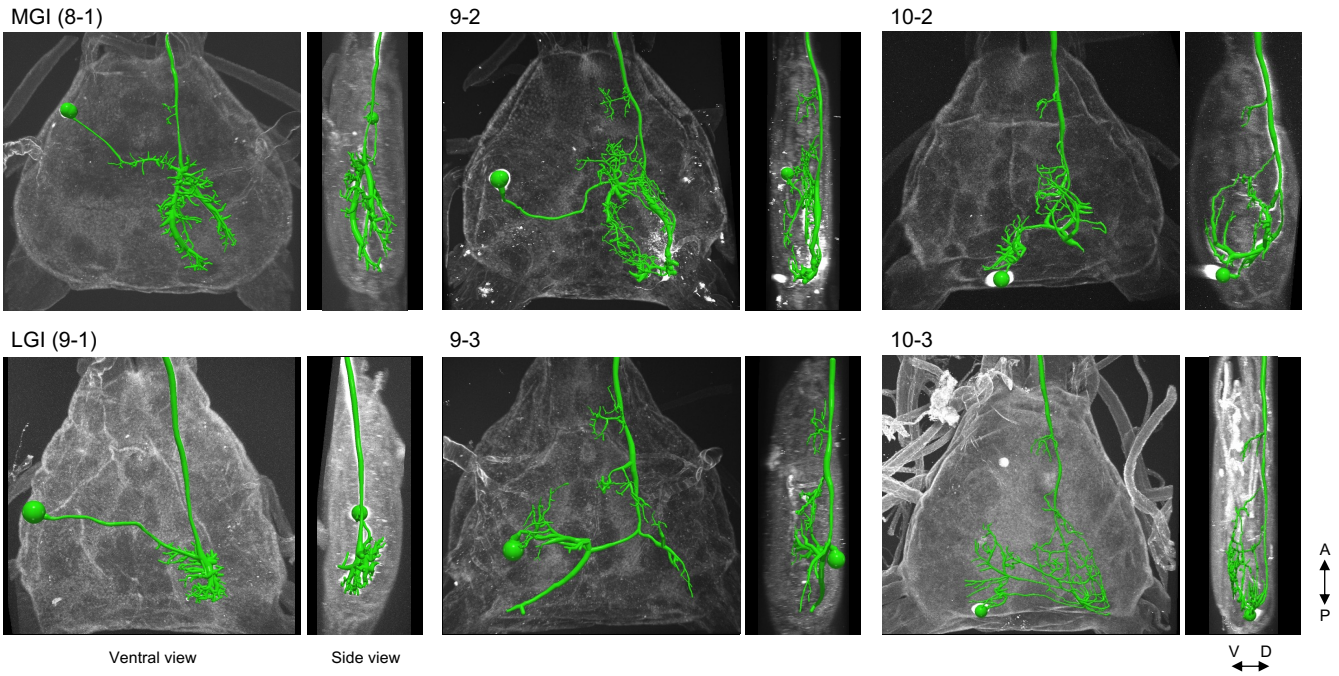

Figure 3

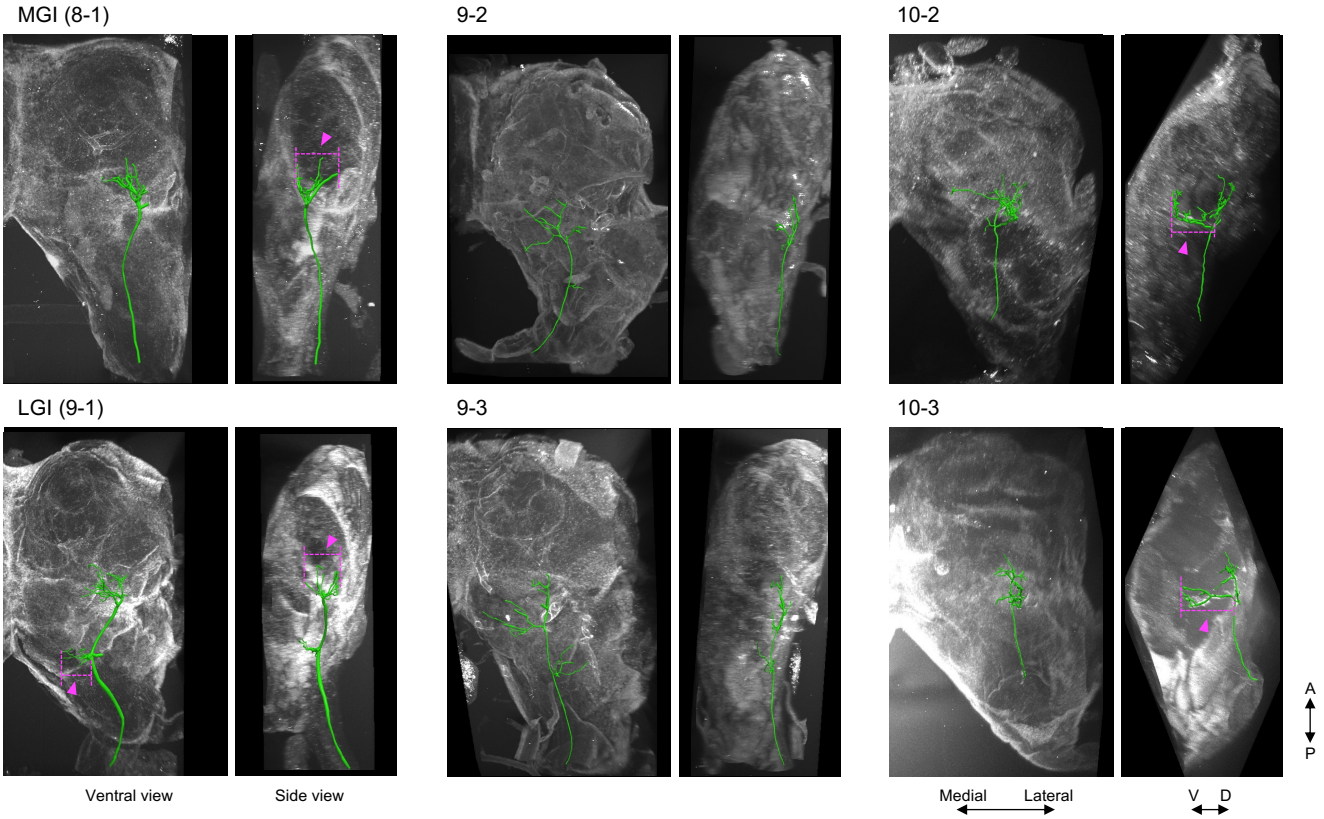
MGI (8-1)
9-2
10-2
LGI (9-1)
9-3
10-3
Ventral view
Side view
Medial
Lateral
V
D
A
P

Figure 4

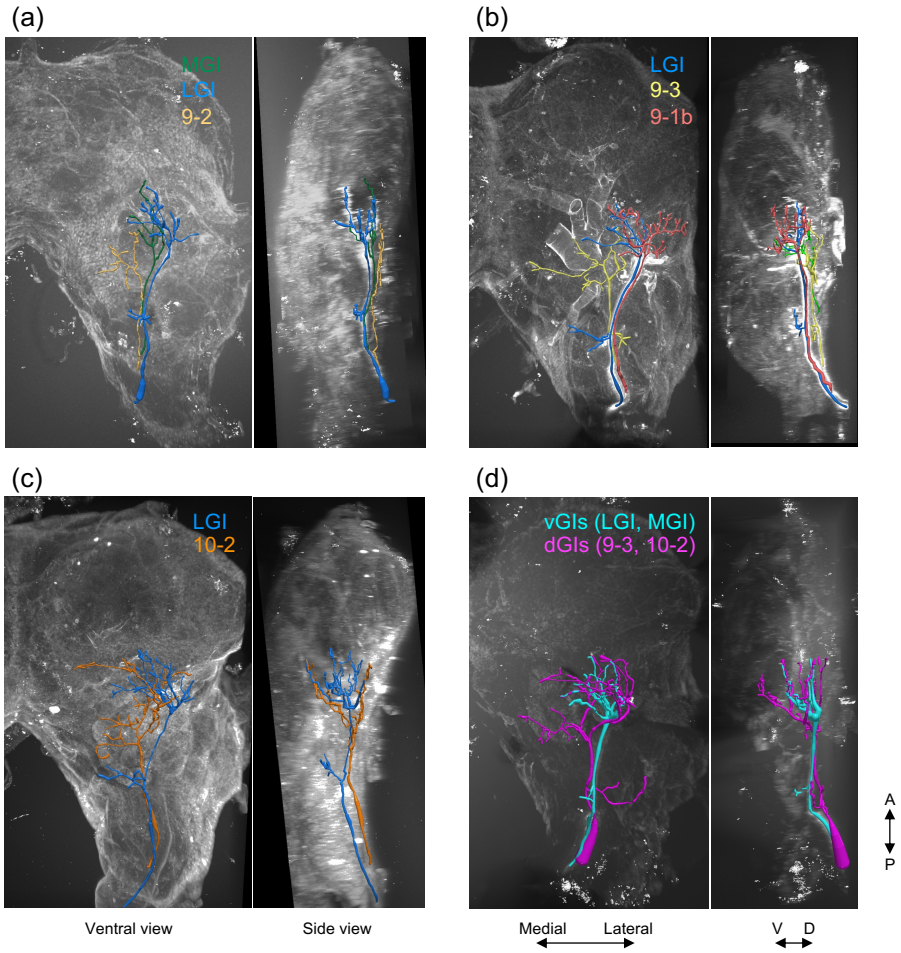
(a)
MGI
LGI
9-2
(b)
LGI
9-3
9-1b
(c)
LGI
10-2
(d)
vGIs (LGI, MGI)
dGIs (9-3, 10-2)
A
P
Ventral view
Side view
Medial
Lateral
V
D

Figure 5

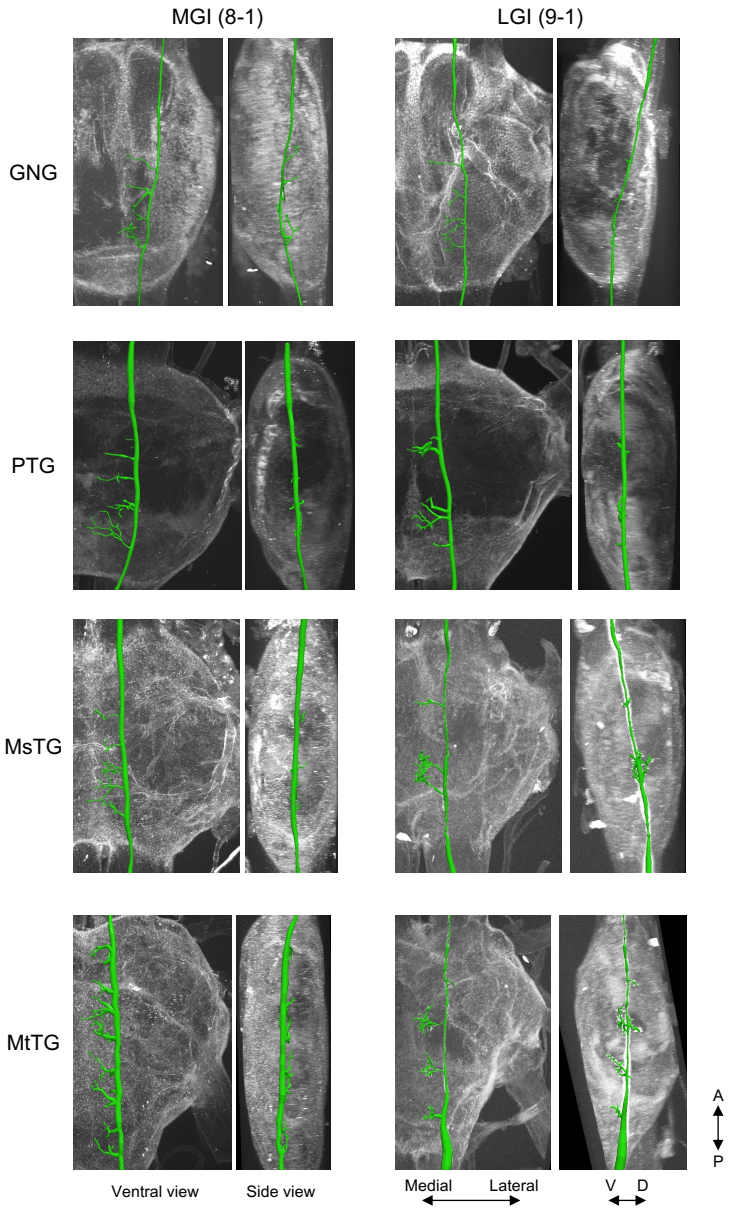
MGI (8-1)
LGI (9-1)
GNG
PTG
MsTG
MtTG
Ventral view
Side view
Medial
Lateral
V
D
A
P

Figure 6

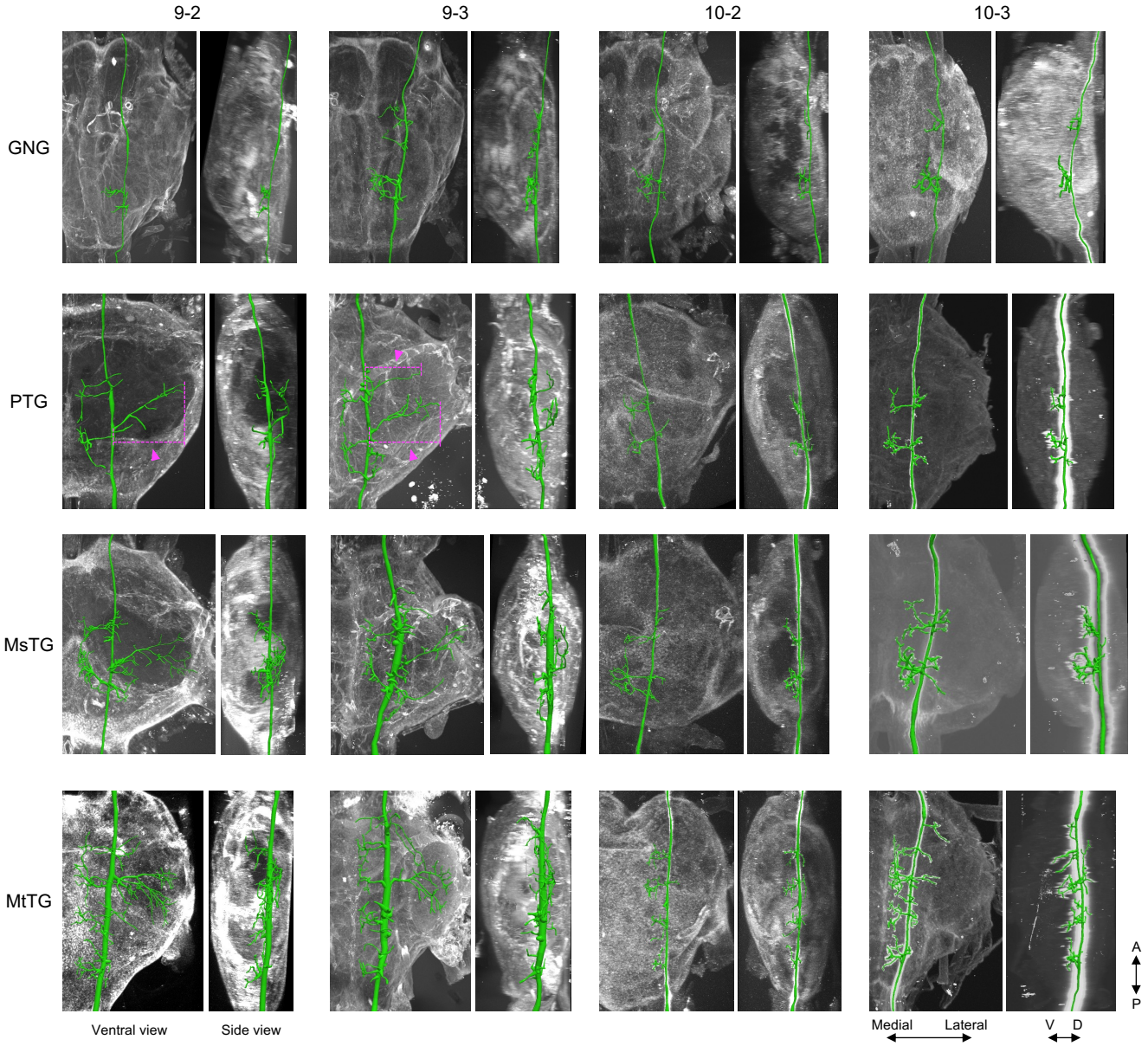
9-2
9-3
10-2
10-3
GNG
PTG
MsTG
MtTG
Ventral view
Side view
Medial
Lateral
V
D
A
P

Figure 7

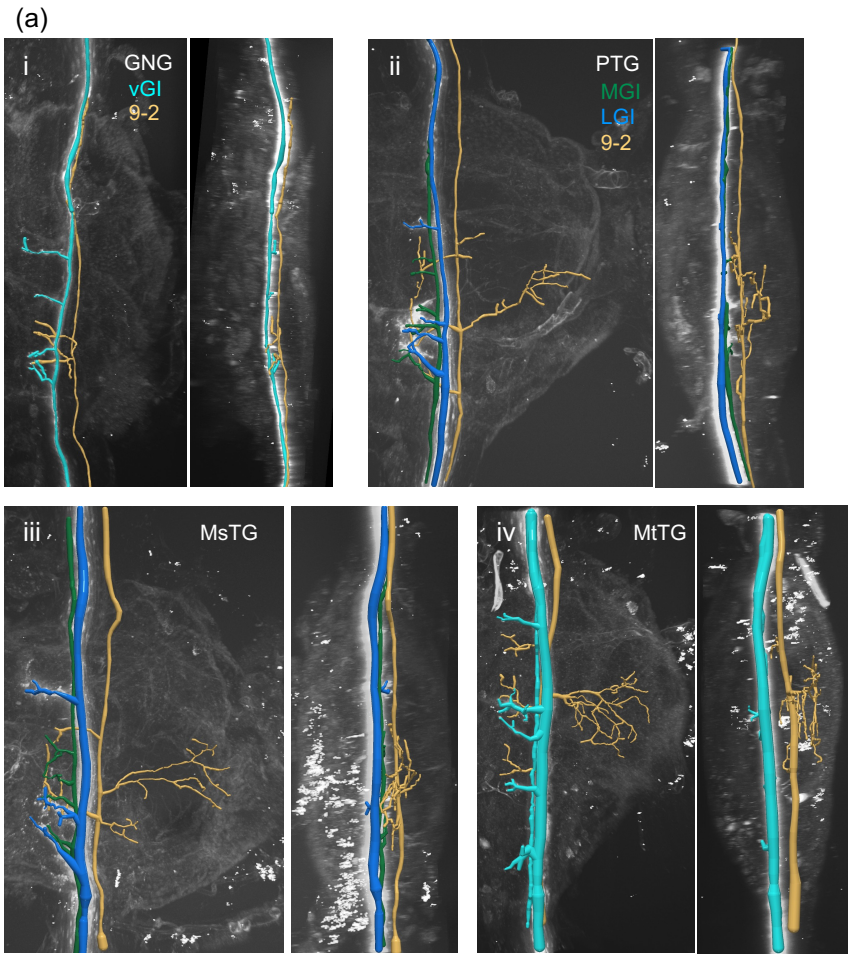
(a)
i
GNG
vGI
9-2
ii
PTG
MGI
LGI
9-2
iii
MsTG
iv
MtTG
(b)
i
GNG
ii
PTG
vGI (LGI, MGI)
dGI (9-3, 10-2)
A
P
Ventral view
Side view
Medial
Lateral
V
D

Table 1. Number of samples analyzed in this study.

		Brain	GNG	PTG	MsTG	MtTG	TAG
Single-cell staining	MGI	2	3	4	3	1	2
	LGI	6	4	8	3	3	4
	GI 9-2	1	3	4	4	4	4
	GI 9-3	5	6	3	2	2	3
	GI 10-2	1	1	1	1	1	3
	GI 10-3	3	4	3	3	2	3
Multiple-cell staining	MGI, LGI	-	-	1	-	-	-
	MGI, GI 9-2	-	1	1	-	1	-
	MGI, GI 10-2	-	-	-	-	-	1
	MGI, GI 10-3	-	1	2	-	1	-
	LGI, GI 9-2	1	-	2	-	-	-
	LGI, GI 9-3	2	3	5	3	-	-
	LGI, GI 10-2	3	1	-	-	-	-
	MGI, LGI, GI 9-2	2	1	1	1	-	-
	MGI, LGI, GI 9-3	1	-	-	-	-	-
	MGI, LGI, GI 9-3, 10-2	1	1	1	-	-	-